Comparative Study between Elliptical Ring and Square Ring Sensor Based on Plasmonic MIM Waveguide

Ashish Varshney[1], Rukhsar Zafar[1, 2], Mohammed Salim[2]
Department of Electronics and Communication Engineering
[1]Swami Keshvanand Institute of Technology, Management & Gramothan, Jaipur
[2]Malviya National Institute of Technology, Jaipur
Email- ashuvarshney27@gmail.com

Abstract: **In this paper, a comparative study between elliptical ring and square ring resonator sensor, coupled to a metal-insulator-metal (MIM) waveguide is theoretically studied and numerically simulated by finite difference time domain (FDTD) method with a perfectly matched layer absorbing boundary condition. Sensing area of elliptical ring and square ring resonator is being made equal. Major and minor radius of elliptical ring resonator are obtained by multiplying a converting factor (k = 0.5643) with outer and inner length of square ring respectively. Some parameters like width of elliptical ring and square ring resonator, refractive index of insulator waveguide and width of insulator waveguide are kept same in both the designs. Silver is taken as metal in MIM structure whose frequency dependent relative permittivity is characterized by Drude model. Variation in resonance wavelength occurs when there is a change in refractive index of material to be sensed. Both the structures are compared for their sensitivity of detecting change in RIU for per change in wavelength. A large value of sensitivity is achieved with square ring resonator when it is compared with elliptical ring resonator. Thus, the square ring resonator can be used in designing highly sensitive refractometer.**

Keywords: **Surface Plasmon Polaritons (SPP), Metal-Insulator-Metal, Refractive Index, Finite-Difference-Time-Domain (FDTD), Drude Model, Sensitivity.**

1. INTRODUCTION

In recent years, a plasmonic based sensor has attracted lots of researchers in this field. In biochemical, these are remarkable tools for analyte detection. For communication industries, the use of photons in sensing makes possible multi dimension and remote interrogation [1]. In plasmonic devices, SPPs are propagating at metal-dielectric interface. Surface Plasmon Polaritons (SPPs) are electromagnetic waves guided along a metal-dialectic interface with amplitude decaying exponentially into both media [2]. SPPs have shown the potential to guide and manipulate light at deep sub-wavelength scale [3]. In the past, SPPs based devices such as the all optical switching [4-6], Mach-Zenhender interferometers [7], splitters [8], modulator [9], mirrors [10], Bragg reflector [11-12] and sensors [13] are simulated numerically and demonstrated experimentally. Refractive index based sensors can be fabricated by either insulator-metal-insulator (IMI) or by metal-insulator-metal (MIM) plasmonic waveguide [13]. The IMI structures are able to propagate over long distance but fail to confine a light into sub-wavelength scale [14]. The MIM waveguides shows a strong confinement of light into sub-wavelength scale with acceptable propagation length for SPPs [11]. Recently, SPPs based sensors has been proposed such as SPP resonance of nano particles [15-16], or enhanced transmission through nanoholes arrays [17-18] to detect change in refractive index of any material. Optical sensing principle utilizes two types of detection techniques such as label-based detection and label-free detection. In label-based detection, to detect and quantify the presence of a specific analyte molecule of interest, target analyte is labeled with either light or fluorescence. In label-free detection, the presence of analyte is reveled by either one of the method such as refractometry, Raman spectroscopy and optical detection of mechanical deflection of movable element. Analyte is not labeled or modified in this type of detection. Using integrated optical devices based on planner waveguide can be implemented by both label-based and label-free sensing scheme. As compared to bulk optic element fiber optic based biochemical sensors with plasmonic sensor possess important advantages [1]. In this paper, two designs such as elliptical ring and square ring resonator based on MIM waveguide have been simulated by FDTD method. In both designs refractive index of elliptical ring and square ring has been varied to observe the variation in the resonance condition. A converting factor (k = 0.5643) is used to calculate parameters for elliptical ring, so that sensing area of both elliptical ring and square ring will be equal. A comparison has been done between elliptical ring and square ring resonator to find out which design offers better sensitivity. A large values of sensitivity are observed (S = 876 nm/RIU) for elliptical ring and (S = 901 nm/RIU) for square ring respectively

2. STRUCTURE AND THEORY

Fig. 1 shows schematic of the elliptical ring resonator. In structure, width of insulator waveguide (d) is 100 nm. Major radius (r_1) is 112.86 nm and minor radius (r_2) is 67.71 nm. Width of elliptical ring resonator is 40 nm. Fig. 2 shows.

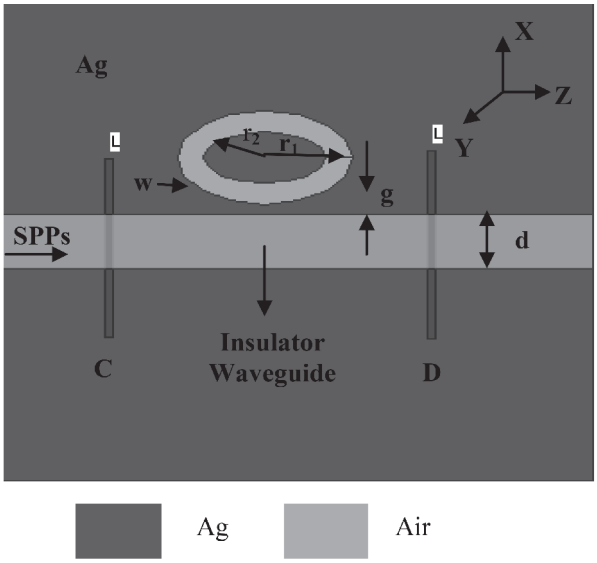

Fig 1: Schematic view of elliptical ring resonator with major radius (r_1) = 112.86 nm, minor radius (r_2) = 67.71 nm, ring width (w) = 40 nm, insulator waveguide width (d) = 100 nm and gap (g) = 20 nm. C & D are observation points

schematic of the square ring resonator. In this structure, outer length of square (a) is 200 nm, inner length (b) is 120 nm and width of square ring (w) is 40 nm. In both design refractive index of insulator waveguide is set as 1.0, which is a refractive index of air. Sensing area of both elliptical ring and square ring

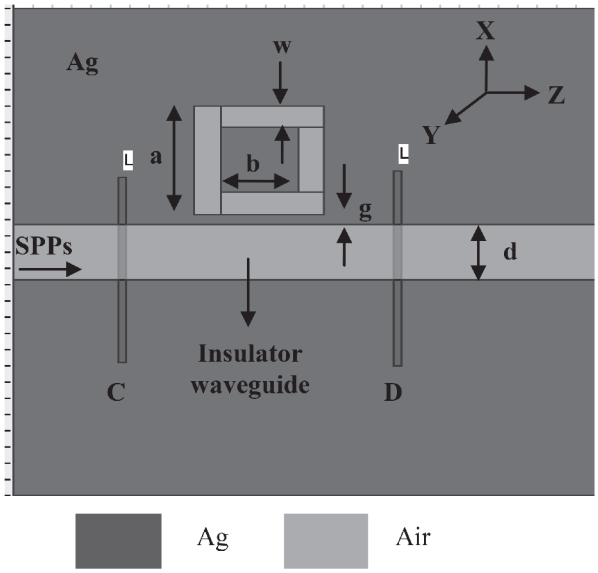

Fig 2: schematic view of a square ring resonator with square outer length (a) = 200 nm, inner length (b) = 120 nm, square width w = 40 nm, insulator waveguide width (d) = 100 nm and gap (g) = 20 nm. C & D are observation points

resonator is equal. By using mathematical equations converting factor (k) is calculated whose value is 0.5643. Major radius (r_1) of elliptical ring resonator is obtained by multiplying outer length (a) of square ring with converting factor (k). Similarly, minor radius of ring resonator is obtained by multiplying inner radius (b) of square ring with converting factor (k). Both elliptical ring and square ring resonator are 20 nm above form insulator waveguide. Elliptical ring and square ring resonator can be fabricated either by electron beam lithography or by conventional lithography [19]. Silver is taken as metal in MIM structure. Frequency dependent permittivity of silver can be governed by Drude model using equation

$$\boldsymbol{\varepsilon(\omega)} = \boldsymbol{\varepsilon_\infty} - \frac{\omega_p^2}{\omega^2 + i\omega\gamma} \quad (1)$$

Where $\varepsilon_\infty = 3.7$, is the interband-transition contribution to the permittivity, $\omega_p = 1.38 \times 10^{16}$ Hz is the bulk plasma frequency and $\gamma = 2.73 \times 10^{13}$ Hz is the electron collision frequency [20]. Both designs are meant to be sense change in refractive index of any liquid or gases material.

3. SIMULATION AND RESULTS ANALYSIS

Both designs are simulated by FDTD (Finite-difference- time-domain) method with perfectly matched layer (PML) boundary condition. PML condition is employed to avoid reflection from the output end of the design. Fundamental TM mode is propagated in insulated waveguide, Because the size of insulating waveguide is very small as compare to input wavelength. SPPs are propagating along the +z axis form left side to right side. Input wavelength is of 1550 nm. Grid sizes for elliptical ring and square ring resonator is 4 x 4 nm in x and z axis respectively. C and D are set as the observation points which observed the reflected power and transmitted power. Formula to calculate transmittance and reflectivity are $T = P_{tr}/P_{in}$ & $R = P_{ref}/P_{in}$ where incident power is denoted by P_{in}.Refractive index of elliptical ring is increased by 0.1 in each step and resonance spectrum is observed. After simulation, it can be seen that increased value of refractive index (η) of elliptical ring produces red shift in resonance wavelength. Resonance wavelength graphs are shown in fig. 3 (a-e). Table 1 shows the values of resonance wavelength in μm for changing refractive index of elliptical ring.

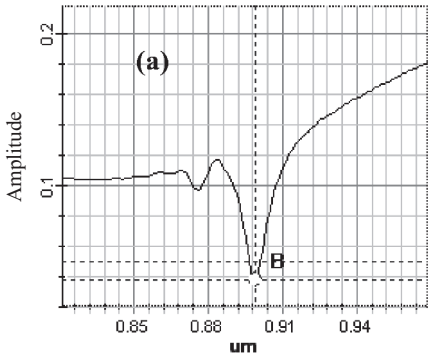

Resonance Wavelength (μm)

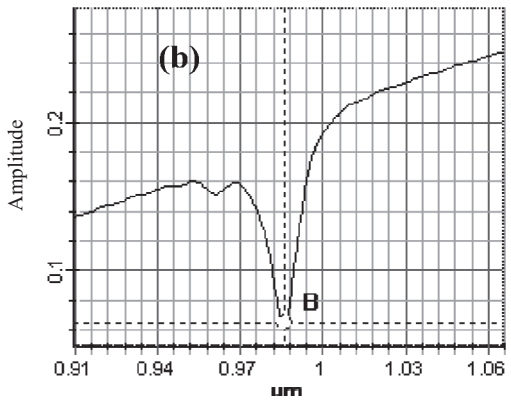

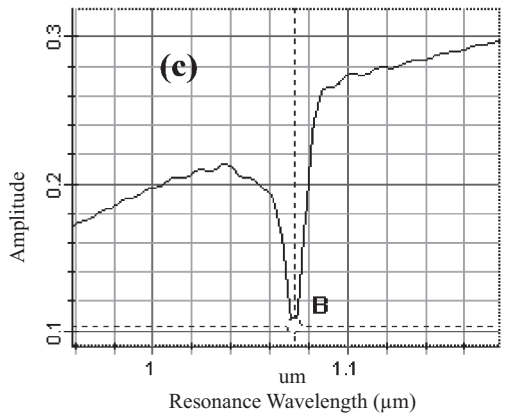

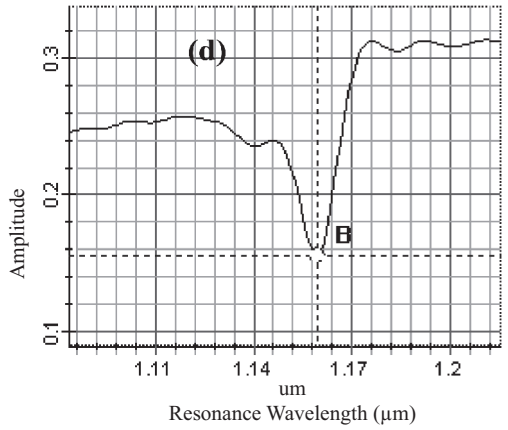

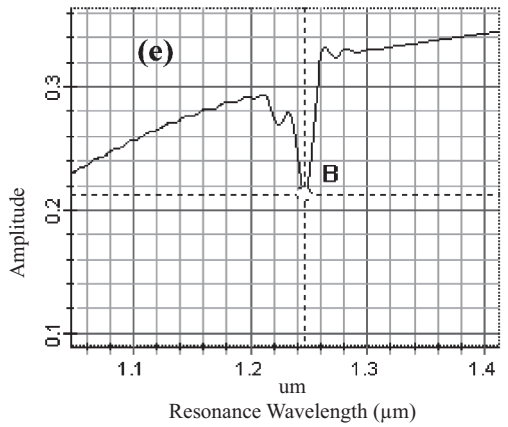

Fig 3: (a-e) shows the transmittance curves when refractive index of elliptical ring resonator is varied from 1.0 to 1.4

Table 1: variation of resonance wavelength with change in refractive index in elliptical ring resonator

Refractive Index of elliptical Ring	Resonance wavelength(μm)
1.0	0.8989
1.1	0.9858
1.2	1.0723
1.3	1.1592
1.4	1.2465

Same procedure is followed to simulate square ring resonator. All the resonance wavelength graphs of square ring are shown in fig 4 (f-j) and table 2 composed of all simulated results

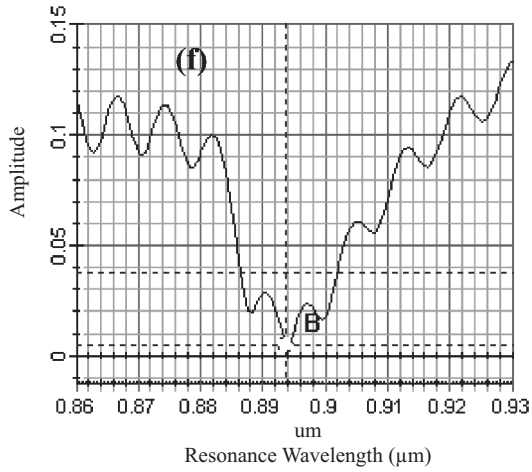

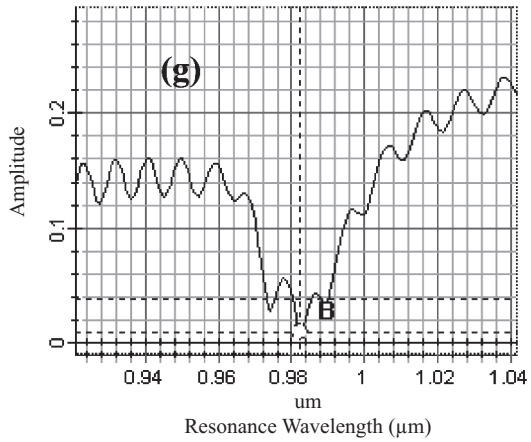

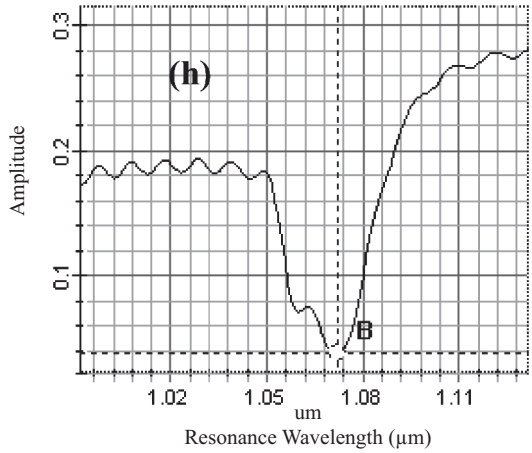

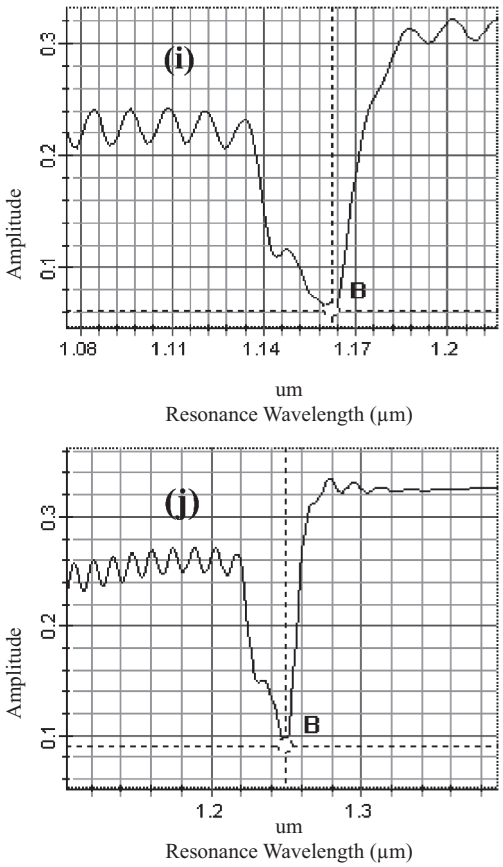

Fig 4: (f-j) shows the transmittance curves when refractive index of square ring resonator is varied from 1.0 to 1.4

Table 2: variation of resonance wavelength with change in refractive index in square ring

Refractive Index of Square Ring	Resonance wavelength(μm)
1.0	0.8937
1.1	0.9824
1.2	1.0721
1.3	1.1622
1.4	1.2489

Spectral sensitivity S [21] is calculated by $S = \Delta\lambda/\Delta\eta$, where $\Delta\lambda$ is a shift in the resonance wavelength and $\Delta\eta$ is a change in the refractive index. Unit for sensitivity is nm/RIU where RIU means refractive index unit. After comparing results of both elliptical ring and square ring resonator, maximum sensitivity is observed in square ring resonator. Maximum sensitivity of elliptical ring and square ring resonator are obtained as 876nm/RIU and 901nm/RIU

4. CONCLUSION

Two designs of highly sensitive refractometer sensors based on MIM waveguide have been proposed. Two designs are elliptical ring and square ring resonator. Both designs are having same sensing area. Any liquid or gaseous material can be filled inside elliptical ring and square ring which is to be sensed. Refractive index can be sensed by these proposed designs. There is a red shift in resonance condition when there is a change in refractive index of material. After comparing both results of proposed design, it is observed that square ring resonator has a high value of sensitivity as compare to elliptical ring resonator. An ultra high value of sensitivity S = 876 nm/RIU for elliptical ring and S = 901 nm/RIU for square ring resonator is achieved.

REFERENCES

[1] Carlos Angulo Barrios, "Optical Slot-Waveguide Based Biochemical Sensors", sensors, vol. 9, pp. 4751-4765, June 2009.

[2] W. L. Barnes, A. Dereux, and T. W. Ebbesen, "Surface plasmon subwavelength optics," Nature, vol. 424, pp. 824–830, 2003.

[3] D. K. Gramotnev and S. I. Bozhevolnyi, "Plasmonics beyond the diffraction limit," Nat. Photon., vol. 4, pp. 83–91, 2010.

[4] C. Janke, J. G. Rivas, P. H. Bolivar, and H. Kurz, "All-optical switching of the transmission of electromagnetic radiation through subwavelength apertures," Opt. Lett., 30(18), 2357–2359 (2005).

[5] C. J. Min, P. Wang, C. C. Chen, Y. Deng, Y. H. Lu, H. Ming, T. Y. Ning, Y. L. Zhou, and G. Z. Yang, "Alloptical switching in subwavelength metallic grating structure containing nonlinear optical materials," Opt. Lett., 33(8), 869–871 (2008).

[6] G. A. Wurtz, R. Pollard, and A. V. Zayats, "Optical bistability in nonlinear surface-plasmon polaritonic crystals," Phys. Rev. Lett., 97(5), 057402 (2006).

[7] B. Wang, and G. P. Wang, "Surface plasmon polariton propagation in nanoscale metal gap waveguides," Opt. Lett., 29(17), 1992–1994 (2004).

[8] G. Veronis, and S. Fan, "Bends and splitters in metal-dielectric-metal subwavelength plasmonic waveguides," Appl. Phys. Lett., 87(13), 131102 (2005).

[9] T. Nikolajsen, K. Leosson, and S. I. Bozhevolnyi, "Surface Plasmon polariton based modulators and switches operating at telecom wavelengths," Appl. Phys. Lett., 85(24), 5833 (2004).

[10] S. Randhawa, M. U. González, J. Renger, S. Enoch, and R. Quidant, "Design and properties of dielectric surface plasmon Bragg mirrors," Opt. Express, 18(14), 14496–14510 (2010).

[11] J. Park, H. Kim, and B. Lee, "High order plasmonic Bragg reflection in the metal-insulator-metal waveguide Bragg grating," Opt. Express, 16(1), 413–425 (2008).

[12] Y. Gong, L. Wang, X. Hu, X. Li, and X. Liu, "Broad-bandgap and low-sidelobe surface plasmon polariton reflector with Bragg-grating-based MIM waveguide," Opt. Express, 17(16), 13727–13736 (2009).

[13] S. Enoch, R. Quidant, and G. Badenes, "Optical sensing based on plasmon coupling in nanoparticle arrays," Opt. Express, 12(15), 3422–3427 (2004).

[14] J. W. Mu, and W. P. Huang, "A Low-Loss Surface Plasmonic Bragg Grating," J. Lightwave Technol., 27(4), 436–439 (2009).

[15] J. J.Mock, D. R. Smith, and S. Schultz, "Local refractive index dependence of plasmon resonance spectra from individual nanoparticles," Nano Lett., vol. 3, pp. 485–491, 2003.

[16] E. M. Larsson, J. Alegret, M. Kall, and D. S. Sutherland, "Sensing characteristics of NIR localized surface plasmon resonances in gold nanorings for application as ultrasensitive biosensors," Nano Lett., vol. 7, pp. 1256–1263, 2007.

[17] A. G. Brolo, R. Gordon, B. Leathem, and K. L. Kavanagh, "Surface plasmon sensor based on the enhanced light transmission through arrays of nanoholes in gold films," Langmuir, vol. 20, pp. 4813–4815, 2004.

[18] A. Lesuffleur, H. Im, N. C. Lindquist, and S.-H. Oh, "Periodic nanohole arrays with shape-enhanced plasmon resonance as real-time biosensors," Appl. Phys. Lett., vol. 90, pp. 243110-1–243110-3, 2007.

[19] H. Ditlbacher, J. R. Krenn, G. Schider, A. Leitner, and F. R. Aussenegg, "Two-dimensional optics with surface plasmon polaritons," Appl. Phys.Lett., vol. 81, pp. 1762–1764, 2002.

[20] Z. H. Han, E. Forsberg, and S. L. He, "Surface plasmon Bragg gratings formed in metal–insulator–metal waveguides," IEEE Photon. Lett., vol. 19, no. 2, pp. 91–93, Jan. 2007.

[21] Leili Abdollahi Shiramin, Reza Kheradmand, and Amin Abbasi, "High-Sensitive Double-Hole Defect Refractive Index Sensor Based on 2-D Photonic Crystal", IEEE sensors Journal, vol. 13, no. 5, pp. 1483-1486, May 2013.

◆ ◆ ◆